Received: 20 January 2020 | Revised: 2 March 2020 | Accepted: 23 March 2020

DOI: 10.1002/jhet.3992

WILEY

ARTICLE

Novel *N*-(benzo[d]oxazol-2-yl)alkanamides; synthesis and carbonic anhydrase II inhibition studies

Aamer Saeed[1] | **Pervaiz A. Channar**[1] | **Muhammad Arshad**[2] | **Hesham R. El-Seedi**[3] | **Qamar Abbas**[4] | **Mubashir Hassan**[5] | **Hussain Raza**[6] | **Sung-Yum Seo**[6]

[1]Department of Chemistry, Quaid-i-Azam University, Islamabad, Pakistan

[2]Chemistry Division Directorate of Science, PINSTECH, Nilore, Pakistan

[3]Pharmacognosy Group, Department of Medicinal Chemistry, Biomedical Center (BMC), Uppsala University, Uppsala, Sweden

[4]Department of Physiology, University of Sindh, Jamshoro, Pakistan

[5]Institute of Molecular Biology and Biotechnology (IMBB), The University of Lahore, Lahore, Pakistan

[6]College of Natural Sciences, Department of Biological Sciences, Kongju National University, Gongju, Republic of Korea

Correspondence
Aamer Saeed, Department of Chemistry, Quaid-i-Azam University, 45320, Islamabad, Pakistan.
Email: aamersaeed@yahoo.com, asaeed@qau.edu.pk

Abstract

Carbonic anhydrase (CA II) inhibitors are very important therapeutic targets in drug design for treatment of neuropathic pain and in eradication of glaucoma, cancer, epilepsy, ulcer and obesity. In this study, some two2-substituted benzoxazoles (**3a-j**) were developed as a new family of carbonic anhydrase II inhibitors by employing acyl thiourea chemistry via a simple and expedient protocol and evaluated for CA II inhibitor activity and radical scavenging ability. Compounds **3f** and **3j** were found to be the most potent inhibitors, with IC_{50} values of 0.00564 and 0.00596 μM, respectively which are several times better than that of the standard, acetazolamide (IC_{50} value 0.997 ± 0.0586 μM). Docking experiments were carried out against the carbonic anhydrase II crystal structure to better rationalize the inhibitory activities of these new structures. Moreover, the results of a DPPH radical scavenging assay showed that the antioxidant profile of compound **3i** is superior to those of other derivatives. The results have revealed that derivatives **3f** and **3j** behave as CA-II inhibitors significantly better than standard and **3i** has good anti-oxidation potential.

1 | INTRODUCTION

Benzoxazole motif is amongst the most important five membered nitrogen oxygen heterocycles fused to a benzene ring exhibiting remarkable pharmacological activities.[1,2] It is found in several naturally occurring bioactive molecules, like UK-1,[3] salvianen,[4] AJI9561,[5] A-33853,[6] caboxamycin,[7] and antimycobacterial pseudopteroxazole.[8] Figure 1 shows examples of some marketed drugs containing benzoxazole motif.

While examples of some bioactive molecules containing benzoxazole from recent literature are mentioned in Figure 2 including the selective peroxisome proliferator-activated receptor γ antagonist JTP-426467,[9c] and the oestrogen receptor-β agonist ERB-041.[9d] Melatonin receptor agonists,[9a] $5HT_3$ receptor agonists,[9b] are some additional examples. Furthermore, benzoxazoles have been widely employed as versatile synthetic building blocks[3,10] in synthesis of insecticides,[11] pharmaceuticals,[12] fluorescent probes,[13] and other functional materials.[14]

Carbonic anhydrases are ubiquitous zinc-metalloenzymes principally responsible for the rapid reversible conversion of CO_2 to bicarbonate.[15–19] In higher vertebrates, 16 isoforms of CA have been identified on the basis of different cellular localizations and tissue distributions.

Present address: Hesham R. El-Seedi, International Research Center for Food Nutrition and Safety, Jiangsu University, Zhenjiang 212013, China; Al-Rayan Research and Innovation Center, Al-Rayan Colleges, 42541, Medina, Saudi.

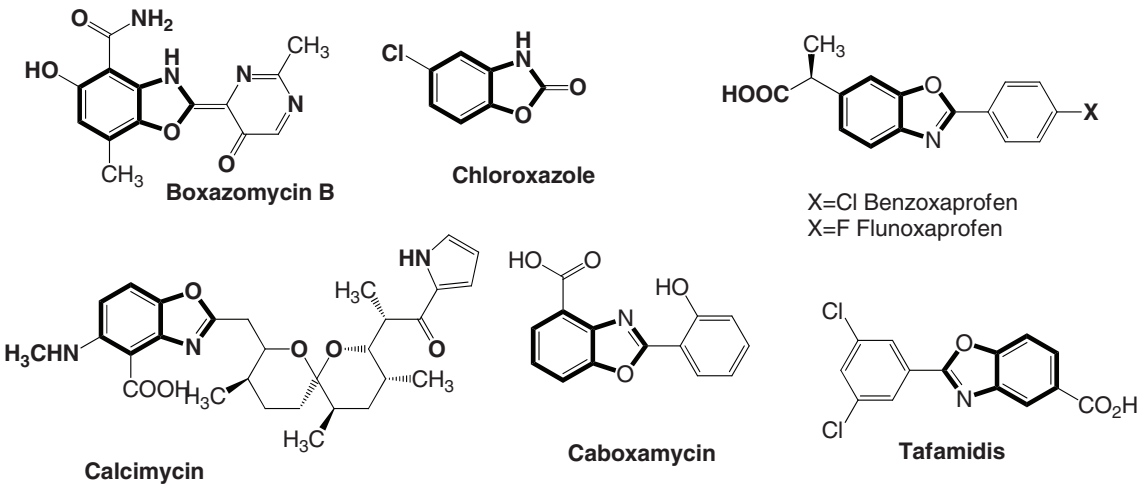

FIGURE 1 Some marketed drugs containing this nucleus

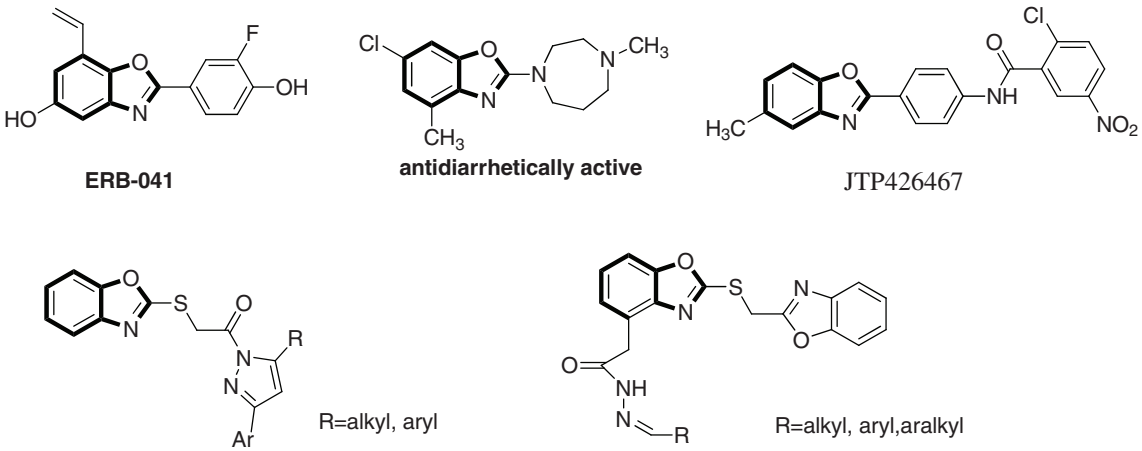

FIGURE 2 Bioactive compounds containing the benzoxazole core

These CA isozymes are involved in various physiological processes, including CO_2 homeostasis, pH regulation, electrolyte secretion, bone resorption and calcification, tumourigenicity, and many other metabolic processes.[15–19] Overexpression of certain CA isozymes may lead to physiological disorders such as hypoxic tumours, gastric ulcers, glaucoma, and obesity.[20] Consequently, CA inhibitors have attracted attention as safe and effective therapeutic agents, and new molecules have been screened by many research groups to identify potent inhibitors of CA.[21]

The presence of amide linkage further increases the biological potential of benzoxazoles. Keeping in view aforementioned importance of benxoxazole and amide linkage, a new series of *N*-(benzo[d]oxazol-2-yl) alkanamides possessing both benzoxazole and amide linkages in a single molecules were prepared in an effort to prepare compounds with better biological potential. The presence of alkyl chains (R) of various lengths confers diversity to these molecules (Figure 3). The ability of these compounds to inhibit carbonic anhydrase II activity was assessed as continuation of our focus to design new classes of CA-II inhibitors.[22,23]

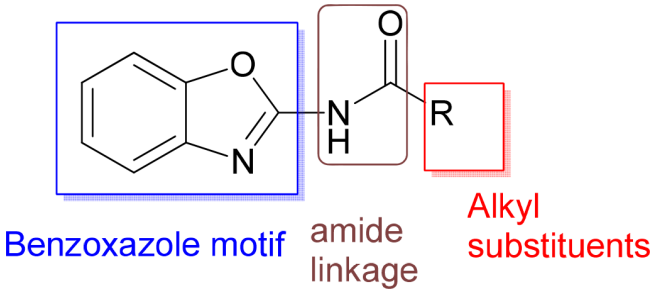

FIGURE 3 Design and architecture of carbonic anhydrase II inhibitors synthesized

2 | MATERIALS AND METHODS

2.1 | Chemistry

All chemicals, reagents, and solvents were purchased from Sigma-Aldrich Chemical Co. or Merck, Germany. The R_f values were determined using aluminium pre-coated silica gel plates Kiesel $60F_{254}$ from Merck (Darmstadt, Germany). The melting points of the compounds were measured in open capillaries using a Stuart melting point apparatus (SMP3). The FTFTIR spectra recorded on FTS 3000 MX, Bio-Rad Merlin (Excalibur Model) spectrophotometer as pure compounds. The ^{1}H and ^{13}C NMR spectra were acquired on a Bruker NMR spectrometer at 300 and 75.5 MHz using TMS as an internal standard. Mass spectra were recorded on an Agilent Technologies 6890 N gas chromatograph equipped with an inert mass selective detector (5973 mass spectrometer), and elemental analyses were conducted using a LECO-183 CHNS analyzer.

2.1.1 | Synthesis of 1-acyl-3-(2-hydroxyphenyl)thioureas (2a-j); general procedure

A solution of suitably substituted acid chloride (3 mmol) in dry acetone (20 mL) was added dropwise to a stirred suspension of potassium thiocyanate (3 mmol) in anhydrous acetone (20 mL). The reaction mixture was stirred at room temperature for 1 hour to afford acyl isothiocyanates (**1a-j**) intermediates. To this a solution of 2-aminophenol (3 mmol) in dry DMF (20 mL) was added, and the resulting mixture was refluxed for 4 to 5 hours. After cooling to room temperature, the reaction mixture was poured onto crushed ice, and the precipitated solid products were filtered off and thoroughly washed. Recrystallization from ethanol afforded (**2a-j**) as coloured crystals.

*1-Acetyl-3-(2-hydroxyphenyl)thiourea (**2a**)*

Brown solid; Yield: 82%; R_f: 0.47 (n-hexane: ethyl acetate, 1:1); m.p.: 119°C to 120°C; FTIR (pure, $\bar{\upsilon}$ cm^{-1}): 3629 (OH), 3273, 3167 (NH), 2960, 2869 ($C_{sp}{}^3$—H), 1685 (C═O), 1560, 1435 (Ar—C═C), 1286 (C═S); ^{1}H-NMR (300 MHz, DMSO-d_6): δ (ppm) 12.73 (s, 1H, CS—NH—CO), 11.31 (s, 1H, Ar—NH—CS), 10.10 (s, broad, 1H, OH), 8.53 (t, 1H, J = 6.9 Hz, Ar—H), 7.11 to 7.07 (m, 1H, Ar—H), 6.93 to 6.88 (m, 1H, Ar—H), 6.84 to 6.80 (m, 1H, Ar—H), 2.42 (s, 3H, $COCH_3$); ^{13}C-NMR (75.5 MHz, DMSO-d_6): δ (ppm) 182.3 (C═S), 175.6 (C═O), 149.1, 129.7, 125.3, 122.2, 121.8, 115.8 (ArCs), 23.4 (CH_3); GC-MS: m/z (%) = 210.05 (100) [$M^{+\cdot}$]; Anal. Calc. for $C_9H_{10}N_2O_2S$: C, 51.41; H, 4.79; N, 13.32; S, 15.25; found: C, 51.43; H, 4.82; N, 13.29; S, 15.27.

*1-(2-Chloroacetyl)-3-(2-hydroxyphenyl)thiourea (**2b**)*

Brown solid; Yield: 78%; R_f: 0.45 (n-hexane: ethyl acetate, 1:1); m.p.: 145°C; FTIR (pure, $\bar{\upsilon}$ cm^{-1}): 3618 (OH), 3270, 3162 (NH), 2924, 2850 ($C_{sp}{}^3$—H), 1682 (C═O), 1568, 1438 (Ar—C═C), 1283 (C═S); ^{1}H-NMR (300 MHz, DMSO-d_6): δ (ppm) 12.60 (s, 1H, CS—NH—CO), 11.22 (s, 1H, Ar—NH—CS), 10.31 (s, broad, 1H, OH), 8.50 (t, 1H, J = 6.9 Hz, Ar—H), 7.07 to 7.03 (m, 1H, Ar—H), 6.95 to 6.90 (m, 1H, Ar—H), 6.83 to 6.78 (m, 1H, Ar—H), 4.23 (s, 2H, CH_2Cl); ^{13}C-NMR (75.5 MHz, DMSO-d_6): δ (ppm) 179.5 (C═S), 177.0 (C═O), 147.8, 131.2, 125.3, 121.1, 121.8, 116.0 (ArCs), 42.9 (CH_2Cl); GC-MS: m/z (%) = 244.01 (100) [$M^{+\cdot}$]; Anal. Calc. for $C_9H_9ClN_2O_2S$: C, 44.18; H, 3.71; N, 11.45; S, 13.10; found: C, 44.22; H, 3.74; N, 11.48; S, 13.09.

*1-(2-Hydroxyphenyl)-3-pivaloylthiourea (**2c**)*

Brown crystalline solid; Yield: 75%; R_f: 0.49 (n-hexane: ethyl acetate, 1:1); m.p.: 125°C to 126°C; FTIR (pure, $\bar{\upsilon}$ cm^{-1}): 3625 (OH), 3267, 3180 (NH), 2958, 2869 ($C_{sp}{}^3$—H), 1688 (C═O), 1575, 1442 (Ar—C═C), 1293 (C═S); ^{1}H-NMR (300 MHz, DMSO-d_6): δ (ppm) 12.43 (s, 1H, CS—NH—CO), 11.05 (s, 1H, Ar—NH—CS), 10.31 (s, broad, 1H, OH), 8.52 (t, 1H, J = 6.9 Hz, Ar—H), 7.06 to 7.01 (m, 1H, Ar—H), 6.93 to 6.88 (m, 1H, Ar—H), 6.81 to 6.77 (m, 1H, Ar—H), 1.24 (s, 9H, $C(CH_3)_3$); ^{13}C-NMR (75.5 MHz, DMSO-d_6): δ (ppm) 185.2 (C═S), 173.9 (C═O), 149.9, 130.7, 126.7, 123.4, 118.7, 115.4 (ArCs), 39.5 ($C(CH_3)_3$), 28.3 ($C(CH_3)_3$); GC-MS: m/z (%) = 252.09 (100) [$M^{+\cdot}$]; Anal. Calc. for $C_{12}H_{16}N_2O_2S$: C, 57.12; H, 6.39; N, 11.10; S, 12.71; found: C, 57.16; H, 6.41; N, 11.13; S, 12.75.

*1-Butyryl-3-(2-hydroxyphenyl)thiourea (**2d**)*

Grey solid; Yield: 79%; R_f: 0.46 (n-hexane:ethyl acetate, 1:1); m.p.: 133°C; FTIR (pure, $\bar{\upsilon}$ cm^{-1}): 3612 (OH), 3269, 3170 (NH), 2937, 2848 ($C_{sp}{}^3$—H), 1660 (C═O), 1577, 1446 (Ar—C═C), 1295 (C═S); ^{1}H-NMR (300 MHz, DMSO-d_6): δ (ppm) 12.52 (s, 1H, CS—NH—CO), 11.47 (s, 1H, Ar—NH—CS), 10.24 (s, broad, 1H, OH), 7.68 (d, 1H, J = 7.0 Hz, Ar—H), 7.54 (dd, 1H, J = 1.8 Hz, Ar—H), 7.30 to 6.77 (m, 2H, Ar—H), 2.41 (t, 2H, J = 6.5 Hz, $COCH_2$), 1.66 to 1.60 (m, 2H, CH_2), 0.84 (t, 3H, J = 6.0 Hz, CH_3); ^{13}C-NMR (75.5 MHz, DMSO-d_6): δ (ppm) 187.8 (C═S), 176.5 (C═O), 150.1, 129.9, 124.3, 122.4, 120.7, 114.5 (ArCs), 38.3 ($COCH_2$), 19.2, 13.1; GC-MS: m/z (%) = 238.08 (100) [$M^{+\cdot}$]; Anal. Calc. for $C_{11}H_{14}N_2O_2S$: C, 55.44; H, 5.92; N, 11.76; S, 13.46; found: C, 55.40; H, 5.89; N, 11.79; S, 13.42.

*1-(2-Hydroxyphenyl)-3-pentanoylthiourea (**2e**)*

Light grey solid; Yield: 85%; R_f: 0.50 (n-hexane:ethyl acetate, 1:1); m.p.: 160°C; FTIR (pure, $\bar{\upsilon}$ cm^{-1}): 3635 (OH), 3272, 3174 (NH), 2924, 2852 ($C_{sp}{}^3$—H), 1669 (C═O), 1580, 1449 (Ar—C═C), 1297 (C═S); ^{1}H-NMR (300 MHz, DMSO-d_6): δ (ppm) 12.76 (s, 1H, CS—NH—CO), 11.31 (s, 1H, Ar—NH—CS), 10.16 (s, 1H, OH), 8.51 (t, 1H, J = 6.0 Hz, Ar—H), 7.07 to 7.01 (m, 1H, Ar—H), 6.93 to 6.90 (dd, J = 6.0 Hz, 1H, Ar—H), 6.83 to 6.78 (m, 1H, Ar—H), 2.45 (t, 2H, J = 9.0 Hz, $COCH_2$), 1.59 to 1.49 (m, 2H, CH_2), 1.36 to 1.24 (m, 2H, CH_2), 0.91 (s, 3H, CH_3); ^{13}C-NMR (75.5 MHz, DMSO-d_6): δ (ppm) 177.7 (C═S), 175.6 (C═O), 149.1, 126.7, 126.3, 123.4, 118.7, 115.4 (ArCs), 35.8 ($COCH_2$), 26.9, 22.1 (CH_2), 14.1 (CH_3); GC-MS: m/z (%) = 252.09 (100) [$M^{+\cdot}$]; Anal. Calc. for $C_{12}H_{16}N_2O_2S$: C, 57.12; H, 6.39; N, 11.10; S, 12.71; found: C, 57.15; H, 6.41; N, 11.13; S, 12.75.

*1-Heptanoyl-3-(2-hydroxyphenyl)thiourea (**2f**)*

Brown solid; Yield: 80%; R_f: 0.39 (n-hexane:ethyl acetate, 1:1); m.p.: 177°C; FTIR (pure, $\bar{\upsilon}$ cm^{-1}): 3645 (OH), 3275, 3181 (NH), 2928, 2856 ($C_{sp}{}^3$—H), 1654 (C═O), 1574, 1445 (Ar—C═C), 1258 (C═S); ^{1}H-NMR (300 MHz, DMSO-d_6): δ (ppm) 12.68 (s, 1H, CS—NH—CO), 11.18 (s, 1H, Ar—NH—CS), 10.60 (s, 1H, OH), 7.69 (d, 1H, J = 6.9 Hz, Ar—H), 7.56 to 7.50 (m, 1H, Ar—H), 7.30 to 7.25 (m, 1H, Ar—H), 6.93 to 6.98 (m, 1H, Ar—H), 2.51 (t, 2H, J = 6.6 Hz, $COCH_2$), 1.58 to 1.45 (m, 2H, CH_2), 1.36 to 1.30 (m, 2H, CH_2), 1.25 (s, 4H, CH_2), 0.90 (s, 3H, CH_3); ^{13}C-NMR (75.5 MHz, DMSO-d_6): δ (ppm) 177.8 (C═S), 175.4 (C═O), 151.9, 130.3, 129.8, 126.5, 123.4, 119.6 (ArCs), 37.3 ($COCH_2$), 31.3, 28.5, 26.0, 22.8 (CH_2), 14.5 (CH_3); GC-MS: m/z (%) = 280.12 (100) [$M^{+\cdot}$]; Anal. Calc. for $C_{14}H_{20}N_2O_2S$: C, 59.97; H, 7.19; N, 9.99; S, 11.44; found: C, 59.99; H, 7.22; N, 9.94; S, 11.46.

*1-(2-Hydroxyphenyl)-3-octanoylthiourea (**2g**)*

Dark brown solid; Yield: 78%; R_f: 0.37 (n-hexane:ethyl acetate, 1:1); m.p.: 198°C to 200°C; FTIR (pure, $\bar{\upsilon}$ cm^{-1}): 3623 (OH), 3280, 3179 (NH), 2927, 2854 ($C_{sp}{}^3$—H), 1693 (C═O), 1580, 1449 (Ar—C═C), 1274 (C═S); ^{1}H-NMR (300 MHz, DMSO-d_6): δ (ppm) 12.75 (s, 1H, CS—NH—CO), 11.59 (s, 1H, Ar—NH—CS), 10.17 (s, 1H, OH), 7.65 (d, 1H, J = 6.8 Hz, Ar—H), 7.27 to 7.21 (m, 1H, Ar—H), 6.86 to 6.80 (m, 1H, Ar—H), 6.77 to 6.71 (m, 1H, Ar—H), 2.50 (t, 2H, J = 6.6 Hz, $COCH_2$), 1.61 to 1.57 (m, 2H, CH_2), 1.30 to 1.36 (m, 2H, CH_2), 1.25 (s, 6H, CH_2), 0.85 (t, 3H, J = 4.4 Hz, CH_3); ^{13}C-NMR (75.5 MHz, DMSO-d_6): δ (ppm) 177.6 (C═S), 171.3 (C═O), 149.1, 126.8, 125.0, 125.0, 122.7, 118.4 (ArCs), 36.1 ($COCH_2$), 31.6, 29.0, 25.7, 24.8, 22.5 (CH_2), 14.3 (CH_3); GC-MS: m/z (%) = 294.14 (100) [$M^{+\cdot}$]; Anal. Calc. for $C_{15}H_{22}N_2O_2S$: C, 61.19; H, 7.53; N, 9.52; S, 10.89; found: C, 61.17; H, 7.55; N, 9.54; S, 10.91.

*1-(2-Hydroxyphenyl)-3-pentadecanoylthiourea (**2h**)*

Light brownish solid; Yield: 74%; R_f: 0.35 (n-hexane:ethyl acetate, 1:1); m.p.: 207°C; FTIR (pure, $\bar{\upsilon}$ cm^{-1}): 3640 (OH), 3267, 3173 (NH), 2930, 2865 ($C_{sp}{}^3$—H), 1678 (C═O), 1572, 1453 (Ar—C═C), 1305 (C═S); ^{1}H-NMR (300 MHz, DMSO-d_6): δ (ppm) 12.70 (s, 1H, CS—NH—CO), 11.55 (s, 1H, Ar—NH—CS), 10.15 (s, broad, 1H, OH), 7.69 (d, 1H, J = 6.8 Hz, Ar—H), 7.22 to 7.17 (m, 1H, Ar—H), 6.84 to 6.78 (m, 1H, Ar—H), 6.76 to 6.70 (m, 1H, Ar—H), 2.30 (t, 2H, J = 6.4 Hz, $COCH_2$), 1.61 to 1.55 (m, 2H, CH_2), 1.28 (s, 22H, CH_2), 0.88 (t, 3H, J = 4.6 Hz, CH_3); ^{13}C-NMR (75.5 MHz, DMSO-d_6): δ (ppm) 175.2 (C═S), 170.5 (C═O), 148.2, 126.7, 125.4, 125.0, 122.5, 118.7 (ArCs), 35.2 ($COCH_2$), 32.2, 29.0, 25.5, 23.9, 22.5 (CH_2), 14.5 (CH_3); GC-MS: m/z (%) = 392.25 (100) [$M^{+\cdot}$]; Anal. Calc. for $C_{22}H_{36}N_2O_2S$: C, 67.30; H, 9.24; N, 7.14; S, 8.17; found: C, 67.33; H, 9.26; N, 7.16; S, 8.19.

*1-(2-Hydroxyphenyl)-3-hexadecanoylthiourea (**2i**)*

Light brownish solid; Yield: 65%; R_f: 0.33 (n-hexane:ethyl acetate, 1:1); m.p.: 215°C; FTIR (pure, $\bar{\upsilon}$ cm^{-1}): 3669 (OH), 3279, 3185 (NH), 2937, 2858 ($C_{sp}{}^3$—H), 1665 (C═O), 1583, 1454 (Ar—C═C), 1217 (C═S); ^{1}H-NMR (300 MHz, DMSO-d_6): δ (ppm) 12.77 (s, 1H, CS—NH—CO), 11.60 (s, 1H, Ar—NH—CS), 10.13 (s, broad, 1H, OH), 7.66 (d, 1H, J = 6.7 Hz, Ar—H), 7.25 to 7.20 (m, 1H, Ar—H), 6.84 to 6.78 (m, 1H, Ar—H), 6.74 to 6.69 (m, 1H, Ar—H), 2.33 (t, 2H, J = 6.4 Hz, $COCH_2$), 1.59 to 1.53 (m, 2H, CH_2), 1.29 (s, 24H, CH_2), 0.87 (t, 3H, J = 4.6 Hz, CH_3); ^{13}C-NMR (75.5 MHz, DMSO-d_6): δ (ppm) 177.4 (C═S), 172.7 (C═O), 148.2, 126.7, 125.4, 125.0, 122.5, 118.4 (ArCs), 37.0 ($COCH_2$), 32.2, 29.0, 25.5, 23.9, 22.5 (CH_2), 13.9 (CH_3); GC-MS: m/z (%) = 406.27 (100) [$M^{+\cdot}$]; Anal. Calc. for $C_{23}H_{38}N_2O_2S$: C, 67.94; H, 9.42; N, 6.89; S, 7.89; found: C, 67.96; H, 9.45; N, 6.93; S, 7.87.

*1-(2-Hydroxyphenyl)-3-stearoylthiourea (**2j**)*

Light brownish solid; Yield: 69%; R_f: 0.32 (n-hexane:ethyl acetate, 1:1); m.p.: 248°C; FTIR (pure, $\bar{\upsilon}$ cm^{-1}): 3649 (OH), 3263, 3178 (NH), 2929, 2850 ($C_{sp}{}^3$—H), 1672 (C═O), 1602, 1437 (Ar—C═C), 1235 (C═S); ^{1}H-NMR (300 MHz, DMSO-d_6): δ (ppm) 12.55 (s, 1H, CS—NH—CO), 10.88 (s, 1H, Ar—NH—CS), 10.10 (s, broad, 1H, OH), 7.67 (d, 1H, J = 6.9 Hz, Ar—H), 7.27 to 7.22 (m, 1H, Ar—H), 6.84 to 6.78 (m, 1H, Ar—H), 6.77 to 6.72 (m, 1H, Ar—H), 2.31 (t, 2H, J = 6.4 Hz, $COCH_2$), 1.60 to 1.54 (m, 2H, CH_2), 1.27 (s, 26H, CH_2), 0.89 (t, 3H, J = 4.7 Hz, CH_3); ^{13}C-NMR (75.5 MHz, DMSO-d_6): δ (ppm) 180.0 (C═S), 173.4 (C═O), 147.7, 127.2, 126.0, 125.1, 122.5, 119.2 (ArCs), 36.9 ($COCH_2$), 32.2, 29.0, 25.5, 23.9, 22.5 (CH_2), 14.1 (CH_3); GC-MS: m/z (%) = 434.30 (100) [$M^{+\cdot}$]; Anal. Calc. for $C_{25}H_{42}N_2O_2S$: C, 69.08; H, 9.74; N, 6.44; S, 7.38; found: C, 69.11; H, 9.76; N, 6.47; S, 7.40.

2.1.2 | Synthesis of *N*-(benzo[d]oxazol-2-yl)alkanamides (3a-j), general procedure

The synthesized thioureas (**2a-j**) were heated above their melting points on a sand bath and evolution of H_2S gas was noticed during fusion. On completion, marked by TLC and cessation of H_2S (in approx.30 minutes). The solid products obtained were cooled to room temperature and purified by re-crystallization from toluene.

N-*(benzo[d]oxazol-2-yl)acetamide (**3a**)*

Dark brown solid; Yield: 69%; m.p.: 160°C to 161°C; FTIR (pure, $\bar{\upsilon}$ cm^{-1}): 3312 (NH), 2939, 2855 ($C_{sp}{}^3$—H), 1658 (C═O), 1568 (C═N); ^{1}H-NMR (300 MHz, DMSO-d_6): δ (ppm) 9.69 (s, broad, 1H, NH), 7.66 to 7.61 (m, 1H, Ar—H), 7.34 to 7.30 (m, 1H, Ar—H), 6.93 to 6.88 (m, 2H, Ar—H), 2.31 (s, 3H, CH_3); ^{13}C-NMR (75.5 MHz, DMSO-d_6): δ (ppm) 168.6 (C═O), 158.2 (C═N), 145.5, 143.3, 123.5, 121.7, 116.0, 108.7 (ArCs), 23.9 (CH_3); GC-MS: m/z (%) = 176.06 (100) [$M^{+\cdot}$]; Anal. Calc. for $C_9H_8N_2O_2$: C, 61.36; H, 4.58; N, 15.90; found: C, 61.32; H, 4.60; N, 15.87.

N-*(benzo[d]oxazol-2-yl)-2-chloroacetamide (**3b**)*

Brown crystalline; Yield: 72%; m.p.: 200°C to 202°C; FTIR (pure, $\bar{\upsilon}$ cm^{-1}): 3309 (NH), 2937, 2858 ($C_{sp}{}^3$—H), 1665 (C═O), 1559 (C═N); ^{1}H-NMR (300 MHz, DMSO-d_6): δ (ppm) 10.82 (s, broad, 1H, NH), 7.68 to 7.63 (m, 1H, Ar—H), 7.33 to 7.29 (m, 1H, Ar—H), 6.95 to 6.91 (m, 2H, Ar—H), 4.20 (s, 2H, CH_2Cl); ^{13}C-NMR (75.5 MHz, DMSO-d_6): δ (ppm) 168.4 (C═O), 155.9 (C═N), 148.4, 142.6, 124.1, 122.8, 115.4, 110.1 (ArCs), 45.2 (CH_2Cl); GC-MS: m/z (%) = 210.02 (100) [$M^{+\cdot}$]; Anal. Calc. for $C_9H_7ClN_2O_2$: C, 51.32; H, 3.35; N, 13.30; found: C, 51.35; H, 3.40; N, 13.22.

N-*(benzo[d]oxazol-2-yl)pivalamide (**3c**)*

Dark brown solid; Yield: 79%; m.p.: 194°C to 196°C; FTIR (pure, $\bar{\upsilon}$ cm^{-1}): 3317 (NH), 2937, 2858 ($C_{sp}{}^3$—H), 1670 (C═O), 1543 (C═N); ^{1}H-NMR (300 MHz, DMSO-d_6): δ (ppm) 10.09 (s, broad, 1H, NH), 7.63 (d, 1H, J = 7.2 Hz, Ar—H), 7.37 (dd, 1H, J = 6.0 Hz, Ar—H), 7.31 to 7.26 (m, 2H, Ar—H), 1.25 (s, 9H, CH_3); ^{13}C-NMR (75.5 MHz, DMSO-d_6): δ (ppm) 170.2 (C═O), 157.2 (C═N), 147.5, 143.3, 122.9, 121.7, 115.8, 109.2 (ArCs), 38.3 ($C(CH_3)_3$), 27.9 ($C(CH_3)_3$); GC-MS: m/z (%) = 218.11 (100) [$M^{+\cdot}$]; Anal. Calc. for $C_{12}H_{14}N_2O_2$: C, 66.04; H, 6.47; N, 12.84; found: C, 66.09; H, 6.52; N, 12.80.

N-*(benzo[d]oxazol-2-yl)butyramide (**3d**)*

Dark brown solid; Yield: 81%; m.p.: 184°C to 186°C; FTIR (pure, $\bar{\upsilon}$ cm^{-1}): 3321 (NH), 2930, 2853 ($C_{sp}{}^3$—H), 1650 (C═O), 1566 (C═N); ^{1}H-NMR (300 MHz, DMSO-d_6): δ (ppm) 9.92 (s, broad, 1H, NH), 7.65 (d, 1H, J = 7.2 Hz, Ar—H), 7.40 (dd, 1H, J = 6.1 Hz, Ar—H), 6.80 to 6.76 (m, 2H, Ar—H), 2.32 (t, 2H, J = 6.0 Hz, $COCH_2$), 1.66 to 1.60 (m, 2H, CH_2), 0.90 (t, 3H, J = 6.1 Hz, CH_3); ^{13}C-NMR (75.5 MHz, DMSO-d_6): δ (ppm) 169.3 (C═O), 154.7 (C═N), 149.5, 144.3, 123.5, 120.9, 114.5, 108.7 (ArCs), 37.6, 19.7 (CH_2), 13.5 (CH_3); GC-MS: m/z (%) = 204.09 (100) [$M^{+\cdot}$]; Anal. Calc. for $C_{11}H_{12}N_2O_2$: C, 64.69; H, 5.92; N, 13.72; found: C, 64.65; H, 5.88; N, 13.77.

N-*(benzo[d]oxazol-2-yl)pentanamide (**3e**)*

Dark brown solid; Yield: 79%; m.p.: 200°C to 201°C; FTIR (pure, $\bar{\upsilon}$ cm^{-1}): 3320 (NH), 2937, 2858 ($C_{sp}{}^3$—H), 1670 (C═O), 1568 (C═N); ^{1}H-NMR (300 MHz, DMSO-d_6): δ (ppm) 9.61 (s, broad, 1H, NH), 7.68 to 7.65 (m, 1H, Ar—H), 7.36 to 7.31 (m, 1H, Ar—H), 6.95 to 6.89 (m, 2H, Ar—H), 4.00 (t, 2H, J = 6.0 Hz, CH_2), 1.74 to 1.65 (m, 2H, CH_2), 1.49 to 1.36 (m, 2H, CH_2), 0.92 (t, J = 6.0 Hz, 3H, CH_3); ^{13}C-NMR (75.5 MHz, DMSO-d_6): δ (ppm) 174.0 (C═O), 158.3 (C═N), 149.1, 144.5, 124.9, 123.4, 115.4, 109.9 (ArCs), 38.1, 26.9, 20.4 (CH_2), 13.0 (CH_3); GC-MS: m/z (%) = 218.11 (100) [$M^{+\cdot}$]; Anal. Calc. for $C_{12}H_{14}N_2O_2$: C, 66.04; H, 6.47; N, 12.84; found: C, 66.07; H, 6.53; N, 12.80.

N-*(benzo[d]oxazol-2-yl)heptanamide (**3f**)*

Grey Solid; Yield: 80%; m.p.: 205°C to 206°C; FTIR (pure, $\bar{\upsilon}$ cm^{-1}): 3314 (NH), 2937, 2858 ($C_{sp}{}^3$—H), 1690 (C═O), 1653 (C═N); ^{1}H-NMR (300 MHz, DMSO-d_6): δ (ppm) 11.05 (s, broad, 1H, NH), 7.60 to 7.54 (m, 1H, Ar—H), 7.33 to 7.29 (m, 1H, Ar—H), 6.74 to 6.69 (m, 2H, Ar—H), 2.03 (t, 2H, J = 6.2 Hz, CH_2), 1.79 to 1.71 (m, 2H, CH_2), 1.45 to 1.33 (m, 6H, CH_2), 0.85 (t, 3H, J = 6.5 Hz, CH_3); ^{13}C-NMR (75.5 MHz, DMSO-d_6): δ (ppm) 167.3 (C═O), 155.9 (C═N), 149.5, 145.3, 125.0, 124.6, 118.5, 110.3 (ArCs), 36.0, 31.6, 28.6, 26.9, 22.3 (CH_2), 13.9 (CH_3); GC-MS: m/z (%) = 246.14 (100) [$M^{+\cdot}$]; Anal. Calc. for $C_{14}H_{18}N_2O_2$: C, 68.27; H, 7.37; N, 11.37; found: C, 68.25; H, 7.40; N, 11.33.

N-*(benzo[d]oxazol-2-yl)octanamide (**3g**)*

Dark brown powder; Yield: 73%; m.p.: 210°C to 212°C; FTIR (pure, $\bar{\upsilon}$ cm^{-1}): 3308 (NH), 2937, 2858 ($C_{sp}{}^3$—H), 1678 (C═O), 1659 (C═N); ^{1}H-NMR (300 MHz, DMSO-d_6): δ (ppm) 9.59 (s, broad, 1H, NH), 7.58 to 7.54 (m, 1H, Ar—H), 7.41 to 7.35 (m, 1H, Ar—H), 6.88 to 6.73 (m, 2H, Ar—H), 2.94 (t, 2H, J = 7.5 Hz, CH_2), 1.60 to 1.56 (m, 2H, CH_2), 1.25 (s, 8H, CH_2), 0.88 (t, 3H, J = 6.5 Hz, CH_3); ^{13}C-NMR (75.5 MHz, DMSO-d_6): δ (ppm) 172.4 (C═O), 157.2 (C═N), 148.3, 141.1, 126.4, 124.5, 119.0, 110.7 (ArCs), 36.3, 31.6, 29.0, 28.9, 24.8, 22.3 (CH_2), 14.4 (CH_3); GC-MS: m/z (%) = 260.15 (100) [$M^{+\cdot}$]; Anal. Calc. for $C_{15}H_{20}N_2O_2$: C, 69.20; H, 7.74; N, 10.76; found: C, 69.22; H, 7.78; N, 10.77.

N-*(benzo[d]oxazol-2-yl)pentadecanamide (**3h**)*

Brown crystalline solid; Yield: 77%; m.p.: 220°C to 222°C; FTIR (pure, $\bar{\upsilon}$ cm^{-1}): 3326 (NH), 2937, 2858 ($C_{sp}{}^3$—H), 1660 (C═O), 1569 (C═N); ^{1}H-NMR (300 MHz, DMSO-d_6): δ (ppm) 11.31 (s, broad, 1H, NH), 7.68 to 7.54 (m, 1H, Ar—H), 7.30 to 7.25 (m, 1H, Ar—H), 6.83 to 6.78 (m, 2H, Ar—H), 2.90 (t, 2H, J = 7.3 Hz, CH_2), 1.61 to 1.55 (m, 2H, CH_2), 1.29 (s, 22H, CH_2), 0.83 (t, 3H, J = 6.0 Hz, CH_3); ^{13}C-NMR (75.5 MHz, DMSO-d_6): δ (ppm) 171.3 (C═O), 157.7 (C═N), 149.1, 141.5, 126.6, 123.9, 119.2, 109.4 (ArCs), 36.7, 32.3, 31.6, 28.6, 27.4, 24.2, 22.3, 20.1 (CH_2), 14.1 (CH_3); GC-MS: m/z (%) = 358.26 (100) [$M^{+\cdot}$]; Anal. Calc. for $C_{22}H_{34}N_2O_2$: C, 73.70; H, 9.56; N, 7.81; found: C, 73.66; H, 9.59; N, 7.84.

N-*(benzo[d]oxazol-2-yl)palmitamide (**3i**)*

Dark brown solid; Yield: 74%; m.p.: 227°C to 229°C; FTIR (pure, $\bar{\upsilon}$ cm^{-1}): 3305 (NH), 2937, 2858 ($C_{sp}{}^3$—H), 1650 (C═O), 1568 (C═N); ^{1}H-NMR (300 MHz, DMSO-d_6): δ (ppm) 9.25 (s, broad, 1H, NH), 7.65 to 7.60 (m, 1H, Ar—H), 7.36 to 7.31 (m, 1H, Ar—H), 6.92 (dd, 2H, J = 8.0 Hz, Ar—H), 2.88 (t, 2H, J = 7.3 Hz, CH_2), 1.58 to 1.46 (m, 2H, CH_2), 1.28 (s, 24H, CH_2), 0.87 (s, 3H, CH_3); ^{13}C-NMR (75.5 MHz, DMSO-d_6): δ (ppm) 166.3 (C═O), 159.5 (C═N), 150.6, 141.8, 126.6, 123.9, 114.6, 109.8 (ArCs), 35.2, 29.3, 22.3, 20.1 (CH_2), 13.8 (CH_3); GC-MS: m/z (%) = 372.28 (100) [$M^{+\cdot}$]; Anal. Calc. for $C_{23}H_{36}N_2O_2$: C, 74.15; H, 9.74; N, 7.52; found: C, 74.17; H, 9.77; N, 7.48.

N-*(benzo[d]oxazol-2-yl)stearamide (**3j**)*

Dark brown solid; Yield: 79%; m.p.: 234°C to 236°C; FTIR (pure, $\bar{\upsilon}$ cm^{-1}): 3315 (NH), 2927, 2849 ($C_{sp}{}^3$—H), 1680 (C═O), 1567 (C═N); ^{1}H-NMR (300 MHz, DMSO-d_6): δ (ppm) 11.59 (s, broad, 1H, NH), 7.58 to 7.54 (m, 1H, Ar-H), 7.30 to 7.24 (m, 1H, Ar—H), 6.90 (dd, 2H, J = 8.0 Hz, Ar—H), 2.46 (t, 2H, J = 6.8 Hz, CH_2), 1.60 to 1.54 (m, 2H, CH_2), 1.23 (s, 28H, CH_2), 0.85 (t, 3H, J = 6.0 Hz, CH_3); ^{13}C-NMR (75.5 MHz, DMSO-d_6): δ (ppm) 166.3 (C═O), 158.3 (C═N), 149.1, 140.9, 126.9, 122.7, 116.3, 110.3 (ArCs), 36.3, 29.4, 25.7, 22.1 (CH_2), 13.9 (CH_3); GC-MS: m/z (%) = 400.31 (100) [$M^{+\cdot}$]; Anal. Calc. for $C_{25}H_{40}N_2O_2$: C, 74.95; H, 10.06; N, 6.99; found: C, 74.99; H, 10.11; N, 6.95.

2.2 | Carbonic anhydrase assay

Carbonic anhydrase inhibition was measured as described previously with some modifications.[24] The method is based on the principle that *p*-nitrophenyl acetate is hydrolysed by carbonic anhydrase to form *p*-nitrophenol, which is yellow colored and can therefore be measured spectrophotometrically. Briefly, the reaction mixture contained 120 μL of 50 mM Tri-sulfate buffer (pH 7.6 containing 0.1 mM $ZnCl_2$), 20 μL of inhibitor and 20 μL (50 U) bovine enzyme per well. Contents were mixed well and pre-incubated at 25°C for 10 minutes. The solution of the substrate, *p*-nitrophenyl acetate, was prepared fresh every time (6 mM stock using <5% acetonitrile in buffer), and 40 μL of fresh solution was added to each well to achieve a final concentration of 0.6 mM. The total reaction volume was 200 μL. After 30 minutes of incubation at 25°C, the contents were mixed, and the absorbance was measured at 348 nm using a microplate reader. Acetazolamide was used as a reference inhibitor, and Tri-sulfate buffer was used as a negative control. Each concentration was analyzed in three independent experiments. The IC_{50} values were calculated by nonlinear regressions using GraphPad Prism 5.0.

$$\text{Inhibition}\,(\%) = [(B-S)/B] \times 100$$

Here, B and S are the absorbance of the blank samples and those with the test compounds, respectively.

2.3 | Free radical scavenging assay

The radical scavenging activities of the test compounds were determined by modifying the method of a reported 2,2-diphenyl-1-picrylhydrazyl (DPPH) assay.[25] The assay solution consisted of 100 mL of 150 mM DPPH, 20 μL of solutions of increasing concentrations of test compounds, and the volume of each was adjusted to 200 μL. The reaction mixtures were then incubated for 30 minutes at room temperature. Ascorbic acid (vitamin C) was used as a reference inhibitor. The measurements were carried out using a micro plate reader (OPTIMax, tunable) at 517 nm. The reaction rates were compared, and the percent inhibition due to the presence of the test compound was calculated. Each concentration was analyzed in three independent experiments.

2.4 | Computational methodology

2.4.1 | Retrieval of carbonic anhydrase II from PDB

The three-dimensional (3D) crystal structure of carbonic anhydrase II was retrieved from the Protein Data Bank (PDB) with PDBID 1V9E (www.rcsb.org). Energy minimization of the target structure was carried out using a conjugate gradient algorithm and an Amber force field in UCSF Chimera 1.10.1.[26] The stereo-chemical properties, Ramachandran graph and values[27] of the carbonic anhydrase II structure were assessed by the MolProbity

server,[28] while the hydrophobicity graph was generated by Discovery Studio 4.1 Client.[29] The protein architecture and statistical proportions of helices, beta sheets, coils and turns were accessed by using the online tool VADAR 1.8.[30]

2.4.2 | In silico design of synthesized compounds and Lipinski's rule validation

The synthesized ligands (**3a-j**) were sketched using the ACD/ChemSketch tool and further minimized by visualizing software (UCSF Chimera 1.10.1). Different online drug assessment tools, such as Molinspiration (http://www.molinspFTIRation.com/) and Molsoft (http://www.molsoft.com/), were employed to predict the drug-likeness and biological properties of these designed candidate molecules. The numbers of rotatable bonds, hydrogen bond acceptors (HBA) and hydrogen bond donors (HBD) were also confirmed by PubChem (https://pubchem.ncbi.nlm.nih.gov/). Moreover, adherence to Lipinski's rule of five was analyzed using Molsoft and MolinspIRaion tools.

2.4.3 | Molecular docking simulation using PyRx

The PyRx docking tool was used to perform molecular docking experiments for all the synthesized ligands (**3a-j**) against carbonic anhydrase II.[31] To perform the docking experiments, grid box dimension values were adjusted to $X = 11.6361$, $Y = 47.8016$ and $Z = 22.1317$. A default exhaustiveness value of 8 was used to obtain the finest binding conformational pose of the protein-ligand docked complexes. All compounds were docked separately against the crystal structure of carbonic anhydrase II. The predicted docked complexes were further evaluated

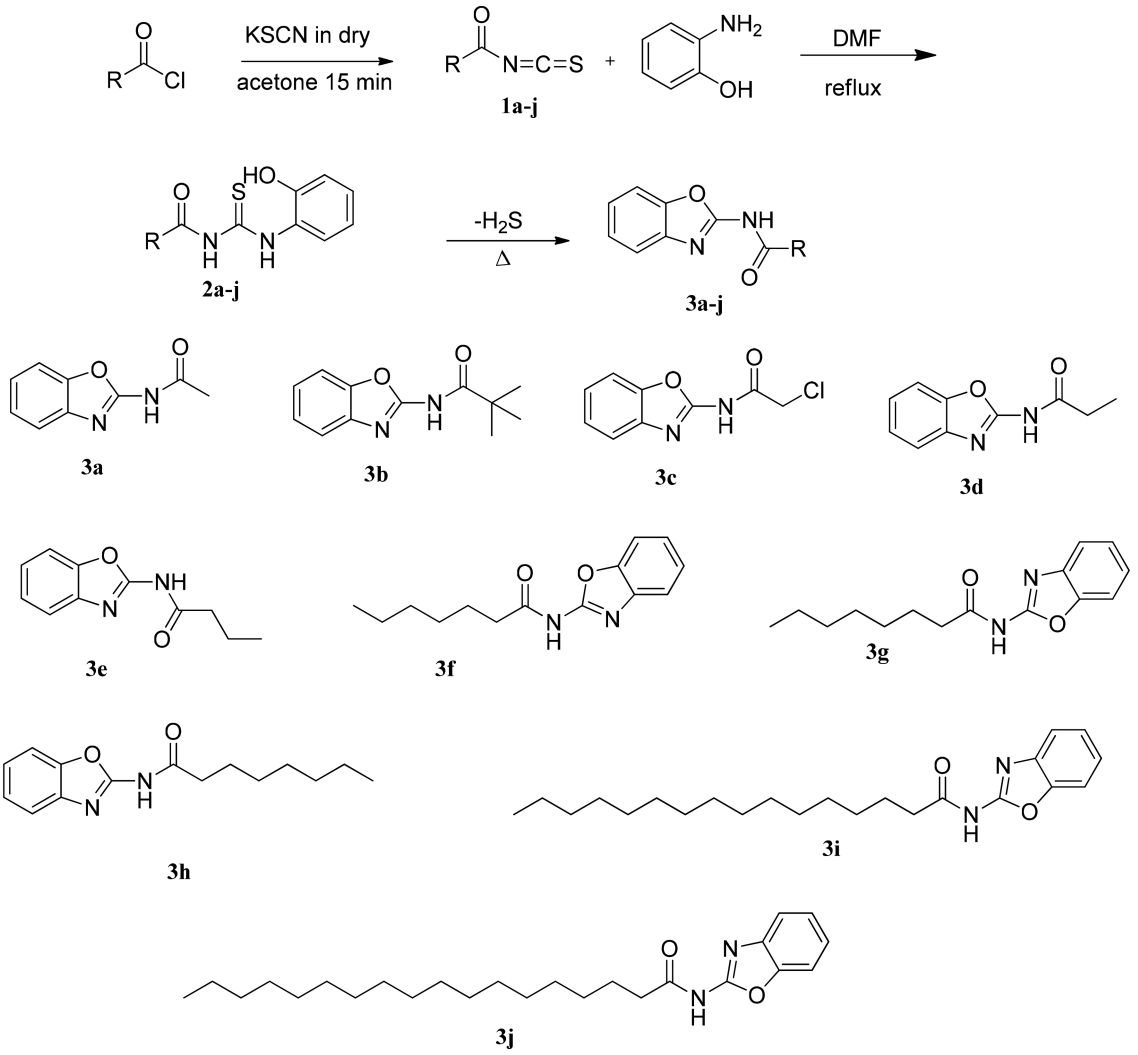

SCHEME 1 Synthetic route and structures of benzoxazoles (**3a-j**)

on the basis of lowest binding energy (kcal/mol) values, and their hydrogen bond and hydrophobic interaction patterns were analyzed using Discovery Studio (4.1) and UCSF Chimera 1.10.1.

3 | RESULTS AND DISCUSSION

3.1 | Chemistry

The strategy adopted for the synthesis of the title compounds is depicted in Scheme 1. Acyl isothiocyanates (**1a-j**) prepared by reaction of corresponding acid chlorides with potassium thiocyanate, in dry acetone, were reacted with *o*-aminophenol in *N,N*-dimethylformamide under reflux to afford 1-acyl-3-(2-hydroxyphenyl)thioureas (**2a-j**). The heterocyclization with concurrent expulsion of the H_2S was achieved by heating thiourea derivatives (**2a-j**) at elevated temperature to furnish the desired *N*-(benzo[d]oxazol-2-yl)alkanamides (**3a-j**) in good yields.

3.2 | Characterization

The elemental analyses and spectral data were in close agreement with the proposed benzoxazole structures. In the FTFTIR spectra of the prepared compounds, the disappearance of the NH and OH peaks and the appearance of absorption peaks in the range 1543 to 1659 cm^{-1} for C═N indicated the cyclization of the thiourea moieties to benzoxazoles. The ^1H NMR spectra of all compounds exhibited a downfield proton for N—H at 9.25 to 11.59 ppm. In the ^{13}C NMR the carbonyl carbon appeared at δ 166.3 to 174.0, while the C═N carbon resonated in the range of 154.7 to 159.5 ppm. The signal at 35.0 to 38.3 ppm was assigned to the CH_2 adjacent to the carbonyl, while the remainder of the carbons appeared in their expected regions.

3.3 | Carbonic anhydrase inhibitory activity

The title compounds (**3a-j**) were screened for in vitro carbonic anhydrase II inhibition activities, and the obtained results are summarized in Table 1. Examination of these data revealed that all newly synthesized benzoxazoles were more potent, with IC_{50} values ranging from 0.00564 to 0.29755 μM, than the standard inhibitor (acetazolamide, IC_{50} = 0.997 μM). The R groups generally appear to influence the CA II inhibitory activities. For instance, the analogues with hexyl and heptadecyl groups (**3f** and **3j**) showed the strongest affinities, with IC_{50} values of 0.00564 and 0.00596 μM, respectively. The compounds with chloromethyl (**3c**; IC_{50} = 0.1466 μM) and propyl (**3d**; IC_{50} = 0.12907 μM) R groups showed weaker affinities. Among the compounds in this series, **3b**, with its bulky *t*-Bu group (IC_{50} = 0.29755 μM), was least active. It seems that the length of the alkyl chain has a significant effect on the enzyme inhibition profile of the tested compounds.

TABLE 1 Carbonic anhydrase inhibitory activities of synthesized compounds **3a-j**

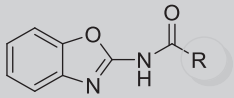

3a-j

Compounds	R	IC_{50} (μM)
3a	CH_3	0.06221 ± 0.00382
3b	$C(CH_3)_3$	0.29755 ± 0.0013
3c	CH_2Cl	0.1466 ± 0.0056
3d	$(CH_2)_2CH_3$	0.12907 ± 0.0085
3e	$(CH_2)_3CH_3$	0.0269 ± 0.0032
3f	$(CH_2)_5CH_3$	0.00564 ± 0.00016
3g	$(CH_2)_6CH_3$	0.0927 ± 0.0024
3h	$(CH_2)_{13}CH_3$	0.0146 ± 0.00094
3i	$(CH_2)_{14}CH_3$	0.06499 ± 0.00298
3j	$(CH_2)_{16}CH_3$	0.00596 ± 0.00021
Acetazolamide		0.997 ± 0.0451

3.4 | Free radical scavenging

All the synthesized *N*-(benzo[d]oxazol-2-yl)alkanamides (**3a-j**) were evaluated for DPPH free radical scavenging ability. The compound **3i** showed good % scavenging potency, other compounds did not show significant radical scavenging potential even at high concentration (100 μg/mL) (Table 2).

3.5 | Structural assessment of carbonic anhydrase II

Carbonic anhydrase II (EC#: 4.2.1.1) is a metal (Zn)-containing protein that comprises 259 residues. The residual architecture of carbonic anhydrase II consists of 9% helices, 45% β sheets and 45% coils. An X-ray diffraction study confirmed its structure to a resolution of 1.95 Å with an R value of 0.238, and unit cell

TABLE 2 Antioxidant activity of synthesized compounds **3a-j**

	DPPH % activity concentrations (μg/mL)							
Compounds	**5**	**10**	**15**	**20**	**40**	**60**	**80**	**100**
3a	35.37	38.95	40.81	43.67	58.52	67.57	73.69	88.27
3b	28.52	30.85	39.11	48.51	61.52	74.43	81.59	93.74
3c	7.21	8.15	9.31	11.81	13.17	16.89	21.04	86.42
3d	21.51	24.61	25.58	32.97	48.75	59.27	67.01	90.91
3e	24.51	26.25	28.34	32.64	45.41	51.63	58.83	83.36
3f	24.41	23.48	25.65	30.65	44.62	52.23	58.71	76.18
3g	23.38	26.94	28.09	30.34	44.37	51.28	57.41	80.72
3h	5.19	8.43	12.56	16.41	22.96	30.26	37.28	43.81
3i	11.03	18.99	23.46	27.25	39.41	54.39	61.58	98.11
3j	7.38	8.16	11.98	12.11	21.21	26.29	31.24	35.36
Vitamin C	45.83	63.51	70.98	81.31	89.22	90.52	94.36	95.97

Note: Results are presented as a mean of n = 3, SEM ± <3%.

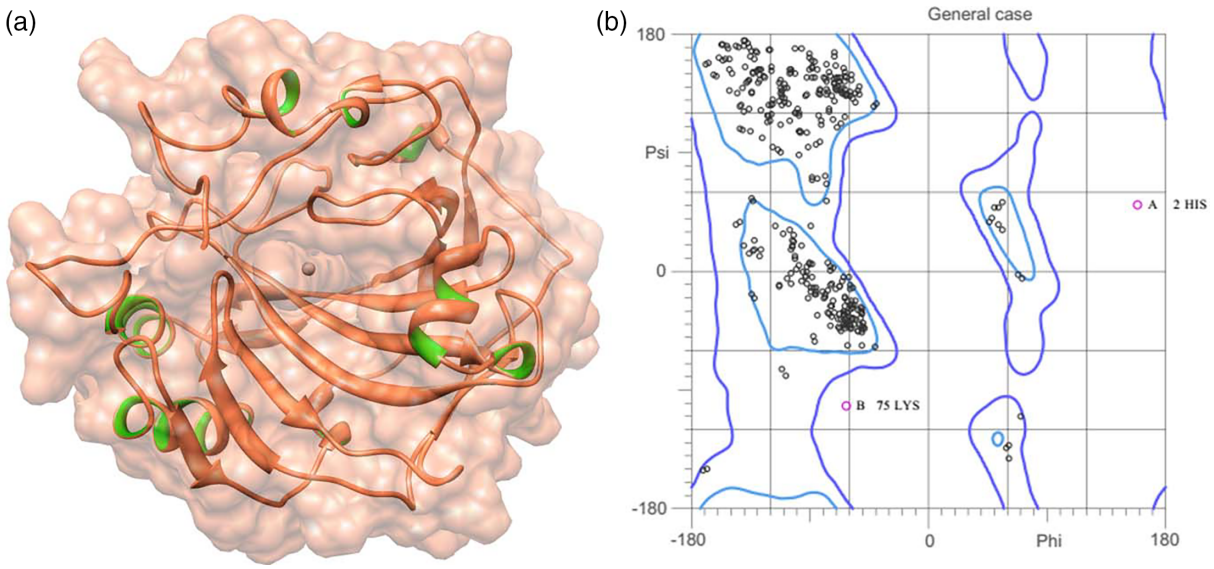

FIGURE 4 A, Crystal structure of bovine anhydrase II. B, Ramachandran graph accessed from PDB

dimensions, such as lengths and angles of coordinates, could be obtained. The computational structure assessment showed that carbonic anhydrase II has unit cell length values of $a = 103.84$, $b = 104.82$ and $c = 119.36$ with angles of 90°, 110.45° and 90° for all α, β and γ dimensions, respectively. Furthermore, the Ramachandran graph and values also confirm the reliability and efficacy of the carbonic anhydrase II structure. The Ramachandran plots indicated that 93.8% of all residues were present in favored regions and that only six rotamers lie in unfavourable regions (Figure 4). The selected Ramachandran graph values showed the good accuracy of the phi (φ) and psi (ψ) angles among the coordinates of the receptor molecules, and most of the residues fell in acceptable regions.

3.6 | Chemo-informatics properties and adherence of the ligands to Lipinski's rule (RO5)

The designed ligands were analyzed computationally to predict the best ligand based on chemical and biomolecular properties and Lipinski's RO5. The predicted chemo-informatics properties, such as Log*P*, HBD, HBA, molar volume, polar surface area (PSA) and drug-likeness values, of the ligand molecules are presented in Table 1. Previous research has confirmed that the standard values for molecular weight (MW) and PSA are 160 to 480 g/mol and (<89 $Å^2$), respectively.[32,33] The predicted results of compounds **3a-j** showed good MW and PSA values that are comparable to the standard values. The

TABLE 3 Chemo-informatics analysis of designed chemical compounds (**3a**-j)

Ligands	Mol. Wt (g/mol)	No. HBA	No. HBD	Mol. Log*P* (mg/L)	PSA (A^2)	Mol.Vol (A^3)	Drug Score
3a	176.06	3	1	1.33	41.89	167.37	−0.58
3b	218.11	3	1	2.54	42.00	232.97	−0.40
3c	210.02	3	1	1.54	41.78	180.22	−0.41
3d	204.09	3	1	2.31	41.78	204.01	−0.21
3e	218.11	3	1	2.79	41.78	221.92	−0.30
3f	246.14	3	1	3.75	41.78	257.73	−0.44
3g	260.15	3	1	4.24	41.78	275.64	−0.44
3h	358.26	3	1	7.61	41.78	400.98	−0.44
3i	372.28	3	1	8.09	41.78	418.89	−0.44
3j	400.31	3	1	9.06	41.78	454.70	−0.44

Abbreviations: HBA, No of hydrogen bond acceptor; HBD, No of hydrogen bond donor; Log*P*, lipophilicity of partition coefficient; LogS, lipophilicity of water; MR, Molar refractivity; PSA, polar surface area; PZ, polarizability.

adherence of these compounds to the RO5 also confirmed their therapeutic potential. Hydrogen-bonding capacity has been identified as an important parameter for describing drug permeability. Poor permeation is more likely to be observed when the number of HBAs and HBDs exceed 10 and 5, respectively.[34,35] The chemo-informatics analysis indicated that all the designed compounds possess <10 HBA and < 5 HBD. Moreover, their Log*P* values were also comparable to the standard values. Compounds **3h**, **3i** and **3j** showed higher values of Log*P*. However, there are many examples of RO5 violations among existing drugs.[36,37] The predicted chemo-informatics values of all the designed ligands are presented in Table 3.

3.7 | Molecular docking and binding energy analysis

Molecular docking experiment is the significant computational approach to study the binding conformation behaviour of ligands against target proteins.[38,39] The docked complexes of all the benzoxazoles (**3a-j**) against CA II were analyzed separately and evaluated on the basis of their minimum energy values and ligand interaction patterns. The results showed that compounds **3b**, **3f**, **3h**, **3i** and **3j** showed good binding energy values of −7.10, −6.70, −7.30, −7.50 and − 7.30 kcal/mol, respectively (Figure 5). Prior research has shown that the SE for Autodock is 2.5 kcal/mol (http://autodock.scripps.edu/).[40] However, in all docking complexes, the predicted energy value difference was less than that of the standard energy. Although the basic core of each synthesized compound was similar, most ligands possess good energy values, and no large energy fluctuations were observed.

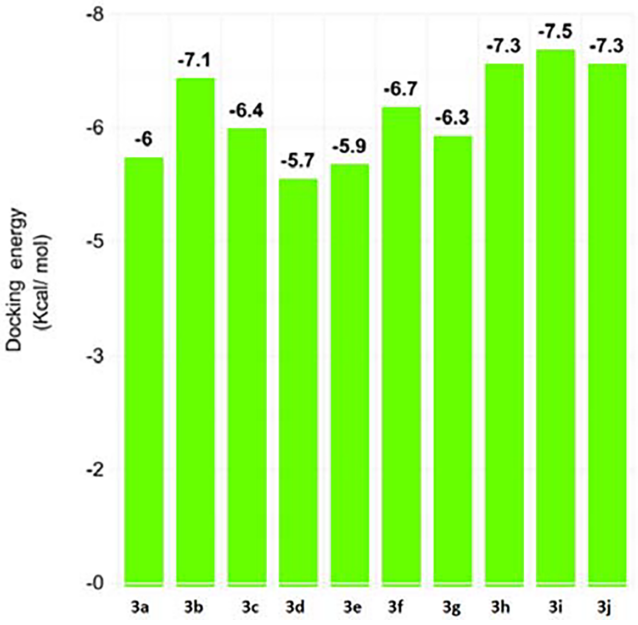

FIGURE 5 Docking energy values of the synthesized compounds (**3a-j**) against the target protein

3.8 | Binding profiles of synthesized compounds against CA II

Based on in vitro and binding energy valued **3f**-CA II docking complex was selected to interpret the binding behavior of synthetic compounds. The ligand-protein binding analyses displayed that **3f** was confined in the active binding pocket of the target protein, as mentioned in Figure 6. CA II has an active site cleft (15 Å in diameter and 15 Å deep) and contains a Zn^{2+} ion that is coordinated in a tetrahedral geometry to three histidine residues (His94, His96 and His119) and a water

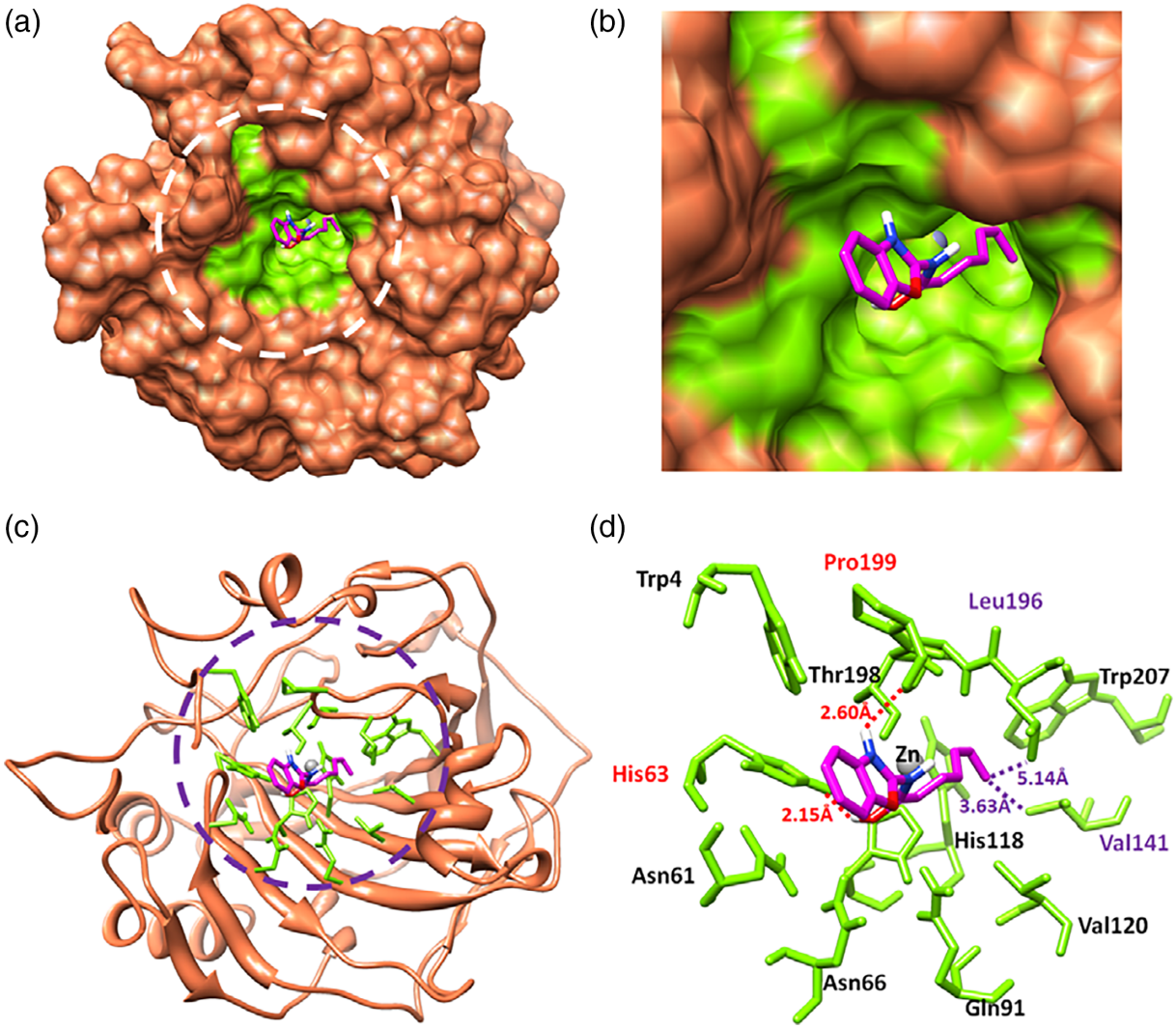

FIGURE 6 Docking interactions 6B with the receptor molecule. A, The general overview of the docking depiction. The surface of the protein structure is represented in brown, while the ligand is highlighted in purple. B, A closer view of the binding pocket interactions with the ligand in the best conformational position. The ligand molecule is depicted in purple, while its functional groups, such as oxygen and amino groups, are shown in red and blue, respectively. C, The docking complex is represented with the ligand conformation. Amino acids are highlighted in green. D, The closer view of the docked complex. The residues involved in hydrogen bonds are shown in red, while residues involved in hydrophobic interactions are labelled in purple with dotted lines showed the interactions, and the distances are given in angstroms (Å). Hydrogen bonds were observed to both His63 and Pro199, while hydrophobic interactions were observed to Val141 and Leu196 in the target protein. Zinc metal is shown in grey

molecule/hydroxide ion.[15] The compound **3f** displayed a good binding conformational position within the CA II binding pocket having hydrogen and hydrophobic interactions. The results of the **3f**-receptor docked complex showed that couple of hydrogen bonds were observed at His63 and Pro199 residual positions. The hydrogen bonds are more significant compared to hydrophobic interaction to interpret the docking complexes. The oxygen moiety in **3f** interacts with His63 with a bond distance of 2.15 Å, while the amide group forms a hydrogen bond to Pro199 having bond length of 2.60 Å.[41] Two hydrophobic interactions were also observed at Val141 and Leu196 having bond lengths of 3.63 and 5.14 Å, respectively.[42] It has been also observed that the bond distances of hydrogen and hydrophobic interactions were also comparable with standard values of bond lengths (<3 and < 5 Å), respectively. The 2D conformation, binding pose and interactions with the binding site residues for all the candidate molecules are presented in Figure S1 to S10.

4 | CONCLUSIONS

In summary, 10 new benzoxazole derivatives have been prepared in very good yields employing a facile and practical synthetic methodology. The compounds (**3a-j**) have

been evaluated for their inhibition of carbonic anhydrase II as well as for their antioxidant capacity. All *N*-(benzo[d]oxazol-2-yl)alkanamides displayed significant micromolar enzyme inhibition activities; compounds **3f** (IC_{50} = 0.00564 μM) and **3j** (IC_{50} = 0.00596 μM) were found to be the most active inhibitors in the series. in silico docking and molecular simulations were performed to understand the binding modes of these benzoxazoles with CA II. The IR drug-likeness scores were estimated, and all compounds obeyed Lipinski's rules. Our preliminary results revealed that compound **3f** showed good drug likeness and might be useful for further biomedical applications.

ACKNOWLEDGEMENTS

We are thankful to the Department of Chemistry, Quaid-i-Azam University Islamabad, Pakistan for providing encouraging environment and facilities for research work. M.F.A. and H.R.E. extend their appreciation to the International Scientific Partnership Program (ISPP) at King Saud University for funding this research work through (ISPP-126).

CONFLICT OF INTEREST

The authors declare no potential conflict of interest.

ORCID

Aamer Saeed https://orcid.org/0000-0002-7112-9296

REFERENCES

[1] Z. P. Yang, C. Zheng, L. Huang, C. Qian, S. L. You, *Angew. Chem.* **2017**, *129*, 1552.

[2] (a)D. Alagille, R. M. Baldwin, G. D. Tamagnan, *Tetrahedron Lett.* **2005**, *46*, 1349. (b) W. Yao, D. Huang, *Org. Lett.* **2010**, *12*, 736. (c) Y. Leng, F. Yang, W. Zhu, Y. Wu, X. Li, *Org. Biomol. Chem.* **2011**, *9*, 5288.

[3] S. Sato, T. Kajiura, M. Noguchi, K. Takehana, T. Kobayashi, T. Tsuji, *J. Antibiot.* **2001**, *54*, 102.

[4] M.-J. Don, C.-C. Shen, Y.-L. Lin, W.-J. Syu, Y.-H. Ding, C.-M. Sun, *J. Nat. Prod.* **2005**, *68*, 1066.

[5] Synthesis and evaluation of new benzoxazole derivatives as potential antiglioma agents Mehlika Dilek ALTINTOP 1 *, Gülşen AKALIN ÇİFTÇİ 2, Halide Edip TEMEL.

[6] S. K. Tipparaju, S. Joyasawal, M. Pieroni, M. Kaiser, R. Brun, A. P. Kozikowski, *J. Med. Chem.* **2008**, *51*, 7344.

[7] C. Hohmann, K. Schneider, C. Bruntner, E. IRran, G. Nicholson, A. T. Bull, A. L. Jones, R. Brown, J. E. Stach, M. Goodfellow, *J. Antibiot.* **2009**, *62*, 99.

[8] (a) A. D. Rodríguez, C. Ramírez, I. I. Rodríguez, E. González, *Org. Lett.* **1999**, *1*(3), 527. (b) J. P. Davidson, E. Corey, *J. Am. Chem. Soc.* **2003**, *125*, 13486–13489.

[9] (a) L.-Q. Sun, J. Chen, K. Takaki, G. Johnson, L. Iben, C. D. Mahle, E. Ryan, C. Xu, *Bioorg. Med. Chem. Lett.* **2004**, *14*, 1197. (b) S. Yoshida, S. Shiokawa, K.-I. Kawano, T. Ito, H. Murakami, H. Suzuki, Y. Sato, *J. Med. Chem.* **2005**, *48*, 7075. (c) J. Nishiu, M. Ito, M. Ishida, T. Kakutani, T. Shibata, M. Matsushita, M. Shindo, *Diabetes Obes. Metab.* **2006**, *8*, 508. (d) L. Leventhal, M. R. Brandt, T. A. Cummons, M. J. Piesla, K. E. Rogers, H. A. Harris, *Eur. J. Pharmacol.* **2006**, *553*, 146.

[10] (a) D. Kumar, M. R. Jacob, M. B. Reynolds, S. M. Kerwin, *Bioorg. Med. Chem.* **2002**, *10*, 3997. (b) J. Kočí, V. Klimešová, K. Waisser, J. Kaustová, H.-M. Dahse, U. Möllmann, *Bioorg. Med. Chem. Lett.* **2002**, *12*, 3275. (c) M. L. McKee, S. M. Kerwin, *Bioorg. Med. Chem.* **2008**, *16*, 1775.

[11] A. Guan, Y. Qin, J. Wang, B. Li, *J. Fluor. Chem.* **2013**, *156*, 120.

[12] (a) R. N. Brown, R. Cameron, D. K. Chalmers, S. Hamilton, A. Luttick, G. Y. Krippner, D. B. McConnell, R. Nearn, P. C. Stanislawski, S. P. Tucker, *Bioorg. Med. Chem. Lett.* **2005**, *15*, 2051. (b) H. Razavi, S. K. Palaninathan, E. T. Powers, R. L. Wiseman, H. E. Purkey, N. N. Mohamedmohaideen, S. Deechongkit, K. P. Chiang, M. T. Dendle, J. C. Sacchettini, *Angew. Chem.* **2003**, *115*, 2864. (c) J. Pan, G.-Y. Liu, J. Cheng, X.-J. Chen, X.-L. Ju, *Eur. J. Med. Chem.* **2010**, *45*, 967.(d) R. F. Sweis, J. A. Hunt, M. L. Hammond, Y. Chen, S. S. Eveland, Q. Guo, S. A. Hyland, D. P. Milot, A.-M. Cumiskey, M. Latham, *Bioorg. Med. Chem. Lett.* **2011**, *21*, 1890.

[13] (a) C.-J. Chen, Y.-C. Wu, H.-S. Sheu, G.-H. Lee, C. K. Lai, *Tetrahedron* **2011**, *67*, 114. (b) M. Taki, J. L. Wolford, T. V. O'Halloran, *J. Am. Chem. Soc.* **2004**, *126*, 712. (c) K. Tanaka, T. Kumagai, H. Aoki, M. Deguchi, S. Iwata, *J. Org. Chem.* **2001**, *66*, 7328.

[14] (a) J. H. Hodgkin, M. S. Liu, B. N. Dao, J. Mardel, A. J. Hill, *Eur. Polym. J.* **2011**, *47*, 394. (b) T. Ogoshi, J. Miyake, Y. Chujo, *Macromolecules* **2005**, *38*, 4425. (c) K. Tamargo-Martinez, S. Villar-Rodil, J. Paredes, A. Martínez-Alonso, J. Tascón, *Chem. Mater.* **2003**, *15*, 4052. (d) C. Wu, P. Tsay, H. Cheng, S. Bai, *J. Appl. Phys.* **2004**, *95*, 417. (e) C.-C. Liao, C.-S. Wang, H.-S. Sheu, C. K. Lai, *Tetrahedron* **2008**, *64*, 7977.

[15] C. T. Supuran, *Nat. Rev. Drug Discov.* **2008**, *7*, 168.

[16] P. Ebbesen, E. O. Pettersen, T. A. Gorr, G. Jobst, K. Williams, J. Kieninger, R. H. Wenger, S. Pastorekova, L. Dubois, P. Lambin, *J. Enzyme Inhib. Med. Chem.* **2009**, *24*, 1.

[17] M. Hilvo, A. M. Salzano, A. Innocenti, M. S. Kulomaa, A. Scozzafava, A. Scaloni, S. Parkkila, C. T. Supuran, *J. Med. Chem.* **2008**, *52*, 646.

[18] M. Falsini, L. Squarcialupi, D. Catarzi, F. Varano, M. Betti, L. Di Cesare Mannelli, B. Tenci, C. Ghelardini, M. Tanc, A. Angeli, *J. Med. Chem.* **2017**, *60*, 6428.

[19] V. Alterio, R. M. Vitale, S. M. Monti, C. Pedone, A. Scozzafava, A. Cecchi, G. De Simone, C. T. Supuran, *J. Am. Chem. Soc.* **2006**, *128*, 8329.

[20] S. Zaib, A. Saeed, K. Stolte, U. Flörke, M. Shahid, J. Iqbal, *Eur. J. Med. Chem.* **2014**, *78*, 140.

[21] G. De Simone, C. T. Supuran, *Curr. Top. Med. Chem.* **2007**, *7*, 879.

[22] R. Qamar, A. Saeed, M. Saeed, Z. Ashraf, Q. Abbas, M. Hassan, F. Albericio, Synthesis, carbonic anhydrase inhibitory activity and antioxidant activity of some 1,3-oxazine derivatives. **2018**, *79*, 352.

[23] S. Pastorekova, S. Parkkila, J. Pastorek, C. T. Supuran, *J. Enzyme Inhib. Med. Chem.* **2004**, *19*, 199.

[24] M. Al-Rashida, M. Ashraf, B. Hussain, S. A. Nagra, G. Abbas, *Bioorg. Med. Chem.* **2011**, *19*, 3367.

[25] F. A. Larik, A. Saeed, P. A. Channar, U. Muqadar, Q. Abbas, M. Hassan, S.-Y. Seo, M. Bolte, *Eur. J. Med. Chem.* **2017**, *141*, 273.
[26] E. F. Pettersen, T. D. Goddard, C. C. Huang, G. S. Couch, D. M. Greenblatt, E. C. Meng, T. E. Ferrin, *J. Comput. Chem.* **2004**, *25*, 1605.
[27] S. C. Lovell, I. W. Davis, W. B. Arendall, P. I. De Bakker, J. M. Word, M. G. Prisant, J. S. Richardson, D. C. Richardson, *Proteins: Struct., Funct., Bioinf.* **2003**, *50*, 437.
[28] V. B. Chen, W. B. Arendall, J. J. Headd, D. A. Keedy, R. M. Immormino, G. J. Kapral, L. W. Murray, J. S. Richardson, D. C. Richardson, *Acta Crystallogr. D Biol. Crystallogr.* **2010**, *66*, 12.
[29] Studio, D., Discovery, version 2.1. Accelrys, San Diego, CA. **2008**.
[30] L. Willard, A. Ranjan, H. Zhang, H. Monzavi, R. F. Boyko, B. D. Sykes, D. S. Wishart, *Nucleic Acids Res.* **2003**, *31*, 3316.
[31] S. Dallakyan, A. J. Olson, *Methods Mol. Biol.* **2015**, *1263*, 243.
[32] R. Kadam, N. Roy, *Indian J. Pharm. Sci.* **2007**, *69*, 609.
[33] A. K. Ghose, T. Herbertz, R. L. Hudkins, B. D. Dorsey, J. P. Mallamo, *ACS Chem. Neurosci.* **2011**, *3*, 50.
[34] M. A. Bakht, M. S. Yar, S. G. Abdel-Hamid, S. I. Al Qasoumi, A. Samad, *Eur. J. Med. Chem.* **2010**, *45*(12), 5862.
[35] A. Saeed, P. A. Mahesar, P. A. Channar, Q. Abbas, F. A. Larik, M. Hassan, H. Raza, S.-Y. Seo, *Bioorg. Chem.* **2017**, *74*, 187.
[36] S. Tian, J. Wang, Y. Li, D. Li, L. Xu, T. Hou, *Adv. Drug Deliv. Rev.* **2015**, *86*, 2.
[37] P. B. Jadhav, A. R. Yadav, M. G. Gore, *Int. J. Pharm. Bio. Sci* **2015**, *6*, 142.
[38] M. Hassan, Z. Ashraf, Q. Abbas, H. Raza, S.-Y. Seo, *Interdiscip. Sci.: Comput. Life Sci.* **2016**, *10*, 1.
[39] M. Hassan, Q. Abbas, Z. Ashraf, A. A. Moustafa, S.-Y. Seo, *Comput. Biol. Chem.* **2017**, *68*, 131.
[40] P. A. Channar, A. Saeed, F. Albericio, F. A. Larik, Q. Abbas, M. Hassan, H. Raza, S.-Y. Seo, *Molecules* **2017**, *22*, 1352.
[41] A. Rauf, M. Raza, M. Saleem, U. Ozgen, E. S. Karaoglan, G. Renda, E. Palaska, I. E. Orhan, *Chem. Biodivers.* **2017**, *14*, e1700024.
[42] K. Sultana, S. Zaib, I. Khan, K. Shahid, J. Simpson, J. Iqbal, *New J. Chem.* **2016**, *40*, 7084.

SUPPORTING INFORMATION

Additional supporting information may be found online in the Supporting Information section at the end of this article.

How to cite this article: Saeed A, Channar PA, Arshad M, et al. Novel *N*-(benzo[d]oxazol-2-yl) alkanamides; synthesis and carbonic anhydrase II inhibition studies. *J Heterocyclic Chem*. 2020;1–13. https://doi.org/10.1002/jhet.3992